



TITLE:

Effects of in vivo cyclic compressive loading on the distribution of local Col2 and superficial lubricin in rat knee cartilage

AUTHOR(S):

Ji, Xiang; Ito, Akira; Nakahata, Akihiro; Nishitani, Kohei; Kuroki, Hiroshi; Aoyama, Tomoki

CITATION:

Ji, Xiang ...[et al]. Effects of in vivo cyclic compressive loading on the distribution of local Col2 and superficial lubricin in rat knee cartilage. *Journal of Orthopaedic Research* 2021, 39(3): 543-552

ISSUE DATE:

2021-03

URL:

<http://hdl.handle.net/2433/263335>

RIGHT:

This is the peer reviewed version of the following article: [Journal of Orthopaedic Research, 39(3), 543-552, March 2021], which has been published in final form at <https://doi.org/10.1002/jor.24812>. This article may be used for non-commercial purposes in accordance with Wiley Terms and Conditions for Self-Archiving.; The full-text file will be made open to the public on 04 August 2021 in accordance with publisher's 'Terms and Conditions for Self-Archiving'.; This is not the published version. Please cite only the published version. この論文は出版社版ではありません。引用の際には出版社版をご確認ご利用ください。

1 **Effects of *in vivo* cyclic compressive loading on the distribution of local Col2 and superficial**
2 **lubricin in rat knee cartilage**

3
4 X. Ji¹, A. Ito^{2*}, A. Nakahata², K. Nishitani³, H. Kuroki², T. Aoyama¹

5
6 ¹Department of Development and Rehabilitation of Motor Function, Human Health Sciences, Graduate
7 School of Medicine, Kyoto University

8 ²Department of Motor Function Analysis, Human Health Sciences, Graduate School of Medicine, Kyoto
9 University

10 ³Department of Orthopaedic Surgery, Graduate School of Medicine, Kyoto University

11
12 Author E-mail addresses

13 gochickenjp@gmail.com (XJ), ito.akira.4m@kyoto-u.ac.jp (AI), akihironakahata@gmail.com (AN),
14 nkohei@kuhp.kyoto-u.ac.jp (KN), kuroki.hiroshi.6s@kyoto-u.ac.jp (HK), aoyama.tomoki.4e@kyoto-
15 u.ac.jp (TA)

16
17 *Corresponding author:

18 Akira Ito
19 53 Shogoin, Kawahara-cho, Sakyo-ku, Kyoto 606-8507, Japan

20 Tel: +81-75-751-3964; Fax: +81-75-751-3964

21 E-mail: ito.akira.4m@kyoto-u.ac.jp

22 Running headline: Cyclic loading affects Col2, lubricin

23 **Abstract**

24 This study aimed to examine the effects of an episode of *in vivo* cyclic loading on rat knee articular
25 cartilage (AC) under medium-term observation, while also investigating relevant factors associated with
26 the progression of post-traumatic osteoarthritis (PTOA). Twelve-week-old Wistar rats underwent one
27 episode comprising 60 cycles of 20 N or 50 N dynamic compression on the right knee joint.
28 Spatiotemporal changes in the AC after loading were evaluated using histology and
29 immunohistochemistry at 3 days and 1, 2, 4, and 8 weeks after loading (n=6 for each condition).
30 Chondrocyte vitality was assessed at 1, 3, 6, and 12 h after loading (n=2 for each condition). A localized
31 AC lesion on the lateral femoral condyle was confirmed in all subjects. The surface and intermediate
32 cartilage in the affected area degenerated after loading, but the calcified cartilage remained intact.
33 Expression of type II collagen in the lesion cartilage was upregulated after loading, whereas the
34 superficial lubricin layer was eroded in response to cyclic compression. However, the distribution of
35 superficial lubricin gradually recovered to the normal level 4 weeks after loading-induced injury. We
36 confirmed that 60 repetitions of cyclic loading exceeding 20 N could result in cartilage damage in the rat
37 knee. Endogenous repairs in well-structured joints work well to rebuild protective layers on the lesion
38 cartilage surface, which may be the latent factor delaying the progression of PTOA.

39

40

41

42

43 **Keywords:** *In vivo* cyclic compression; Post-traumatic osteoarthritis; Cartilage degeneration; Rat model;

44 Type II collagen; Superficial lubricin

45 Introduction

46 Post-traumatic osteoarthritis (PTOA) is a classification of clinical osteoarthritis (OA) that is common
47 among patients with a history of articular cartilage (AC) damage and ligament injury. Animal models play
48 an important role in understanding the pathophysiology of PTOA as well as developing novel therapies to
49 treat this disease. Small animals such as rodents have the advantage of a faster pathological process and
50 lower maintenance costs compared to large animals; hence, rodents are widely used as PTOA models for
51 experimental purposes. The anterior cruciate ligament transection (ACLT) and destabilization of the
52 medial meniscus (DMM) were the optimal conditions for short-term studies in the past. In recent decades,
53 non-surgical models have been considered instead in order to avoid surgery-induced inflammation that
54 could affect the evaluation. One of the most promising candidates is cyclic compression on knee AC¹.

55

56 The *in vivo* cyclic compression model was first designed for verifying trabecular bone adaptation to
57 mechanical loading²⁻⁴ and was developed as a nonsurgical model of OA in later studies⁵⁻¹². However, there
58 are doubts regarding the accuracy of the simulated pathologic progression of clinically relevant secondary
59 OA in these models. One problem was over-frequent loading, which contributed to excessive subchondral
60 bone reaction and the formation of disproportionately giant osteophytes, reported in many cases^{7,8,12}. Ko
61 et al¹¹ reported a single session of loading induced OA-like morphological destruction, where the regimen
62 comprised 1200 cycles, roughly equal to the 5 days/week design in other studies. Poulet et al⁵ confirmed
63 that a loading episode of 60 cycles induced AC lesions without osteophyte formation, but after monitoring
64 for 2 weeks found no loss in Safranin O staining. Therefore, further study on long-term tracking of low-
65 dose loading effectiveness is necessary.

66

67 Although earlier studies using cyclic compression models showed visible osteophytes and reduced
68 substrate staining, none reported irregular wearing of cartilage surface or subchondral bone porosity loss,
69 which are important characteristics of OA progression in surgery-induced rodent OA models^{13,14}. Thus,
70 depending on the magnitude of compressive loading and the methodology of joint instability surgery, the
71 mechanisms of repair or alleviation of the AC lesion in OA progression are still unclear.

72

73 The current study aimed to track the relatively long-term effect of *in vivo* low-dose cyclic loading on rat
74 knee joints, the first such study in rat species. Further, we examined changes over time in loading-affected
75 cartilage and investigated potential causes for the slower progression of OA development in a non-surgical
76 model relative to a surgical model.

77

78 **Methods**

79 *Mechanical loading procedures and sample allocation*

80 All experimental procedures were approved by the animal research committee of Kyoto University
81 (approval number: Med kyo 17616). Seventy-four 12-week-old wild-type male Wistar rats were used in
82 this study. The animals were anesthetized with 5% isoflurane solution (Pfizer, Tokyo, Japan) before being
83 injected intraperitoneally with 1 µg/g somnopentyl (Kyoritsu Seiyaku Corp., Tokyo, Japan). Each animal's
84 right knee was fixed with a customized cup with approximately 140 degrees flexion, as previously
85 described⁶, and subjected to one session of dynamic loading in the daytime using a measuring compression
86 instrument (Autograph AG-X, Shimazu, Japan). The loading regimen included a preload of 5 N and peak
87 load of 20 N or 50 N, with approaching speed of 1 mm/s and 10 s rest intervals (Figure 1A-B). The load
88 levels were set according to previous studies in other species^{6,9}, and were proportionately amplified based

89 on animal weight. Each session comprised 60 cycles that lasted approximately 12 min total. After loading
 90 compression, animals were returned to transparent plastic cages with a 12-h light/dark cycle and provided
 91 adequate feed and free space for movement. Experimental rats were randomly divided into three groups
 92 (peak load 20 N or 50 N, and control). The rats (n=6 for each condition, n=60 in total) were sacrificed for
 93 histological analysis at 3 days and 1, 2, 4, and 8 weeks after compression. Knee samples that underwent
 94 20 N loading were harvested at 1, 3, 6, and 12 h for the live/dead assessment of chondrocytes (n=2 for
 95 each timepoint, n=8 in total). Normal 12-week old Wistar rat samples served as controls (n=4) for
 96 histological analysis and controls (n=2) for cell viability evaluation (Figure 1C). Randomization was
 97 performed using Excel functions, and animals in different experimental groups were treated in random
 98 order each time.

99

100 *Live/dead analysis of chondrocytes*

101 To evaluate the live/dead spatiotemporal changes of chondrocytes on lateral femoral condyles, calcein
 102 AM/ethd-1 staining (LIVE/DEAD Viability/Cytotoxicity Kit, Thermo Fisher Scientific, Tokyo, Japan)
 103 was performed immediately after specimens were dissected from the knee joints. Samples were treated
 104 with calcein AM (diluted 1:500) and Ethd-1 (diluted 1:4000) solutions in PBS for 20 min at room
 105 temperature. Samples were then rinsed in PBS and cut into two parts of the femoral intercondylar sulcus.
 106 The lateral half was then mounted on a transparent plate with the femoral condyle towards the camera
 107 (Supplementary figure 1). Fluorescence micrographs were taken using a fluorescence microscope
 108 (Fluoview FV10i, Olympus, Tokyo, Japan) with FITC (495/519 nm) and PI (535/617 nm) channels. Live
 109 cells were indicated by green fluorescence, and dead cells by red fluorescence. Contralateral limbs
 110 harvested at 12 h were used as controls.

111

112 *Histological analysis*

113 Knee joints were fixed in 4% paraformaldehyde overnight and decalcified in 10% EDTA for 25 days.
114 Samples were then embedded in paraffin. Twelve 6- μ m sagittal sections for every 100- μ m interval were
115 prepared, covering the entire area of the lesion in the lateral femur for each sample. Safranin O, fast green,
116 and hematoxylin staining were performed on each section, and the average modified Mankin score¹⁵ was
117 calculated to evaluate the degree of cartilage degeneration at the lateral femoral condyle. To assess the
118 volume of degenerative cartilage, the lesion area was defined using ImageJ software, and the stacked
119 volume was calculated by multiplying the total area by a 100- μ m average thickness. The intensity of
120 Safranin O staining was calculated on an inverted 8-bit grayscale image using ImageJ software. The
121 relative intensity in lesion areas was calculated by dividing by the intensity in normal cartilage
122 (Supplementary figure 2). In addition, the hematoxylin-stained nuclei of chondrocytes in the lesion
123 cartilage were counted.

124

125 *Immunohistochemistry and semi-quantitative evaluation*

126 Immunohistochemical staining of type II collagen (Fine Chemical Co., Toyama, Japan; diluted 1:200),
127 matrix metalloproteinase thirteen (MMP-13) (ab39012 Abcam Co., Tokyo, Japan; diluted 1:1000), A
128 disintegrin and metalloproteinase with thrombospondin motifs five (ADAMTS-5) (ab185795 Abcam Co.,
129 Tokyo, Japan; diluted 1:50), and Lubricin/Proteoglycan 4 (EMD Millipore, Temecula, USA; diluted
130 1:1000) were performed as described below. Deparaffinized sections were treated with 3% hydrogen
131 peroxide solution for 30 min. Sections were then stained for the anti-type II collagen reaction and treated
132 with 1.25% hyaluronidase for 60 min at room temperature. Sections for the ADAMTS-5 reaction were

133 treated with HistoVT One solution (Nacalai Tesque, Inc., Kyoto, Japan; diluted 1:10) for 40 min at 65 °C.
134 After rinsing in PBS, nonspecific reactions were suppressed by blocking with 5% normal goat serum for
135 60 min. Subsequently, sections were treated with primary antibodies and incubated at 4 °C overnight.
136 Sections were then washed in PBS and treated with goat anti-rabbit IgG (MMP-13 and ADAMTS-5) or
137 goat anti-mouse IgG (type II collagen and lubricin) for 30 min at room temperature. Detection was
138 performed using the streptavidin–biotin–peroxidase complex technique with an Elite ABC kit (diluted
139 1:100; Vector Laboratories, Burlingame, CA, USA). Localization was detected using 3,3-
140 diaminobenzidine solution (Vector Laboratories) followed by counterstaining with hematoxylin.

141
142 Immunohistological staining in the cartilage matrix of type II collagen and lubricin was evaluated using
143 ImageJ software. Images were converted to grayscale (0–255) from dark to bright, and intensity was
144 calculated by subtracting the values in blank spaces. Details of ROI selection are described in
145 Supplementary figure 3. The number of MMP-13- and ADAMTS-5-positive immunostained
146 chondrocytes in the lesion area and the adjoining zone were counted and normalized by dividing by the
147 corresponding cartilage surface length. The adjoining zone was defined as the area in proximity to the
148 lesion cartilage in a 0.48 mm × 0.64 mm 200× histological image.

149
150 *Statistical analysis*

151 Statistical analyses were performed using SPSS software (version 22.0; SPSS Inc., Chicago IL). Two-way
152 analysis of variance was employed to analyze histological staining with loading as intragroup factors and
153 duration as intergroup factors. The normality of all continuous data was examined using the Shapiro–Wilk
154 normality test. The parametric variables of the modified Mankin score, volume of degenerative areas, and

155 semi-quantitative measurements of immunohistochemistry were included in the model directly, whereas
156 the nonparametric variables were first transformed into ranked data and then introduced into the model.
157 Comparisons between intergroup marginal means using Tukey HSD tests were performed only when the
158 main effects exhibited significant results. When the analysis showed interactional effects in addition to
159 the significant main effects, multiple one-way ANOVA tests with post-hoc comparisons for stratified
160 samples were conducted on each level to examine potential differences in interactional effects among the
161 levels. Additionally, Mann-Whitney U (2 groups) or Kruskal-Wallis H tests (3 groups) were applied to
162 compare the control and loaded samples. The required sample size was calculated based on our pilot
163 experimental data of lesion area size between groups. P-value < 0.05 was considered statistically
164 significant.

165

166 **Results**

167 *Vitality of chondrocytes after cyclic loading*

168 Samples that underwent 20 N cyclic compression were stained with calcein AM/ethd-1 and evaluated
169 (Supplementary figure 4). Representative images exhibited mixed distribution of red and green fluorescent
170 cells at 1 and 3 h after loading, whereas large areas without green-stained chondrocytes were observed at
171 6 and 12 h, indicating that complete cell death occurred within 6 h, even at the lower load level of 20 N.

172

173 *Degree and extension of the articular cartilage lesion*

174 Histology showed that AC in both groups was damaged, and one focal degenerative zone in the lateral
175 femoral condyle was confirmed for every subject (Supplementary figure 4A). However, the AC surface

176 remained intact except for a slight fibrillation present in several samples (data not shown). A clear
 177 boundary between the lesion cartilage and unaffected calcified cartilage was observed 2 weeks after
 178 loading. The average modified Mankin score per section increased after loading (Supplementary figure
 179 4F) and differed between groups and observational durations (Supplementary figure 4B). As the peak load
 180 or interval time increased, the degree of degeneration tended to worsen at higher histological scores
 181 (Supplementary figure 4B). Although the lesion area volume did not change significantly throughout the
 182 duration of the study, it was significantly higher in the 50 N load group than in the 20 N group at all time
 183 points (Supplementary figure 4C). The relative Safranin O staining intensity in the lesion area declined
 184 with time after loading for both groups compared to the intact area (Supplementary figure 4D); however,
 185 there was no evident difference between groups with 20 N or 50 N peak loads. In addition, the number of
 186 hematoxylin-stained nuclei in the lesion area continuously decreased after loading in both groups
 187 (Supplementary figure 4E, 4G), whereas no significant changes were found in medium-term observation
 188 from 2 to 8 weeks.

189

190 *Expression of type II collagen in the lesion area*

191 Immunohistochemistry results showed focal type II collagen overexpression in the AC lesion. Enhanced
 192 staining was observed in each sample compared to adjacent intact substrates (Figure 3A), and the intensity
 193 in loaded samples was significantly higher than in the control group (Figure 3B). However, there were no
 194 notable effects on intensity in the lesion region with different load levels or time points (Figure 3C-D),
 195 regardless of whether raw values or relative percentage increments were used.

196

197 *Distribution of ADAMTS-5- and MMP-13-positive chondrocytes*

198 Superficial and intermediate zone chondrocytes in the control group moderately expressed MMP-13 and
 199 ADAMTS-5 (Supplementary figure 5). In the loading groups, we found positively stained radial zone
 200 chondrocytes under the lesion area (Supplementary figure 6, Figure 4) that were not observed in normal
 201 samples (quantitative data not shown). The number of active cells in the area adjoining the lesion (no
 202 direct contact) significantly increased after loading compared to normal AC (Supplementary figure 6B,
 203 Figure 4B). Moreover, the results of semi-quantitative analysis revealed that the number of both MMP-
 204 13- and ADAMTS-5-positive chondrocytes (in the lesion area or in the adjoining region) gradually
 205 decreased during the 8-week observation period (Supplementary figure 6C-D, Figure 4C-D). However,
 206 no significant main effects were generated by the load levels.

207

208 *Superficial lubricin response to cyclic loading*

209 Lubricin expression in the lateral femoral condyle AC is presented in Figure 5. The staining intensity in
 210 the lesion area of substrates within the superficial cartilage declined one week after loading compared to
 211 that in the intact area (Figure 5A). However, semi-quantitative analyses showed an increased
 212 concentration of lubricin on the AC lesion over time, reaching the same level at 4 and 8 weeks compared
 213 to the intact area (Figure 5B). No statistical load-level effect was found, whereas the main effects of
 214 duration and interaction between observational duration and load effect were confirmed. Furthermore,
 215 results of stratified analysis revealed that superficial lubricin in 20 N-loaded samples were more likely to
 216 recover (more pairwise differences) in comparison to 50 N samples (Figure 5C-D). Additionally, we found
 217 signs of stain aggregating around the site of degenerative chondrocytes or even lacunae from dead cells
 218 lacking hematoxylin-stained nuclei.

219

220 Discussion

221 The current study demonstrated for the first time that a single episode comprising 60 cycles of mechanical
222 stimulus can induce AC lesions in the lateral femoral condyle of rats, consistent with results reported in
223 smaller rodents such as mice⁵⁻⁶. Compared to surgical PTOA models of ACLT and DMM that gradually
224 develop chondrocyte apoptosis and cartilage matrix loss¹⁶, we did not find any apoptotic cells around the
225 lesion area, even at 6 h after loading (data not shown). This was considerably different from previous
226 results in mice showing that clustered active TUNEL-stained chondrocytes were retained in degenerative
227 AC until 14 days after loading⁶. Our results from live/dead staining demonstrate that chondrocytes in the
228 superficial lesion cartilage were dead within 6 h due to direct damage (Figure 2). The Mankin score¹⁵
229 deteriorated over time, whereas structural destruction of AC cartilage did not progress as rapidly as the
230 invasive models that showed a jagged cartilage surface and subchondral bone perforation within 4 weeks
231 after the instability surgery^{17,18}. Furthermore, there was a distinct difference in staining between AC above
232 and below the tidemark (Supplementary figure 4A), consistent with *in vitro* results indicating that calcified
233 radial zones of cartilage suffered less than 5% of the total mechanical stress^{19,20}. Cell signaling studies
234 have suggested that overloading activates the toll-like receptors expressed on chondrocytes, resulting in
235 the release of inflammatory cytokines²¹ and catalyzing ADAMTS-5 for aggrecan degradation²², consistent
236 with findings of the current study (Supplementary figure 6). According to our investigation, this non-
237 surgical model may be superior for simulation of acute extensive AC damage, which is common in athletic
238 injuries.

239

240 Expression of Col2 was found to be transiently increased within 1 h after *ex vivo* mechanical loading in
241 several experiments using extracted cartilage explants^{23,24}. A recently published tissue-engineering
242 review²⁵ summarized the biochemical anabolism of synthetic substrate-seeded chondrocytes subjected to

243 *in vitro* dynamic loading, most of which demonstrated subsequent Col2 upregulation in response to
244 various loading regimens. Ragan²³ reported transient upregulation of type II collagen within 4 h in
245 extracted bovine cartilage explants subjected to static mechanical compression but did not check the
246 chondrocyte survival rate. The current study, to our knowledge, is the first report on focal enhanced
247 staining of type II collagen in lesion cartilage that has undergone *in vivo* cyclic loading, despite the
248 complete death of the affected surface chondrocytes within 6 h. A previous study reported decreased
249 Safranin O and Col2 staining in an osteochondral defect model²⁶, which was directly created on the AC
250 surface using a 1-mm biopsy punch. However, our model showed a diametrically opposite type-II-
251 collagen response to cyclic loading. Although one of the major collagenases, MMP-13, was overexpressed
252 immediately after loading injury (Figure 4), the morphological degradation of AC did not progress
253 extensively as in regular OA development. Further studies should focus on whether type II collagen
254 proliferation is beneficial or harmful to AC protection.

255

256 Lubricin localized on the cartilage surface is reportedly a protective and lubricating component of the *O*-
257 linked glycoprotein²⁷. We found drastic decrease in superficial lubricin staining of the damaged area
258 immediately after cyclic loading compared with the non-loaded region (Figure 5). Decreased superficial
259 cartilage lubricin/proteoglycan 4 was confirmed in both *in vivo*²⁸ and *ex vivo*²⁹ experiments. Several
260 studies have reported an increased coefficient of friction within a few hours of cyclic loading^{30,31} and that
261 lubricin in the cartilage surface was denuded by loading, even in the joint where most chondrocytes
262 remained alive throughout the observation period³¹. Our study revealed similar results in a non-surgical
263 model during early observation after *in vivo* cyclic compression. On the other hand, after tracking different
264 time points for 8 weeks, we found that superficial cartilage staining with lubricin gradually recovered to
265 the normal level (Figure 8). The results after 4 weeks indicated a different trend of OA progression

266 compared to that with joint instability-induced OA. Although lubricin expression on cartilage was found
267 to be elevated in late-stage OA patients³², mainstream results from posttraumatic OA of human³³ and
268 animal joint instability models^{28,34-36} in a long-term observation demonstrated that joint lubricin
269 concentration decreased after injury or surgery. Combining our results with the results of decreased *Prg4*
270 expression in unstable joints after forced movement,^{37,38} we hypothesized that instability-induced
271 persistent motivation should play a more important role than magnitude of loading in determining
272 irreversible lubricin loss. Several studies^{35,39,40} involving delivery of exogenous recombinant lubricin to
273 medial meniscectomized rats found that the cartilage surface protein was protected from depletion in the
274 experimental group. In the current study, we observed a self-healing process in the loading-damaged AC
275 without any lubricin supplementation, indicating that endogenous lubricin is an important repair
276 mechanism in the post-traumatic knee and providing a plausible explanation regarding the slower cartilage
277 degradation progression in the non-invasive loading model compared to that in the joint instability surgery
278 models. Interestingly, although superficial cell death was confirmed within 6 h after loading, the locations
279 of cartilage lacunae were strongly stained with lubricin even at 8 weeks after injury. Previous studies
280 found that chondrocytes encapsulated in agarose^{20,41} and cartilage explants⁴² expressed higher levels of
281 *prg4* when subjected to compressive strain and the intensified lacunae staining around cells was confirmed
282 by immunofluorescence images²⁰, similar to our results. Further studies should focus on potential links
283 between chondrocyte-derived lubricin and the mechanism of superficial cartilage repair.

284

285 The current study has some limitations. First, it focused on investigating the medium-term changes over
286 time from 3 days to 8 weeks after loading implementation. Since cell death, type II collagen biosynthesis,
287 and superficial lubricin degradation occurred earlier than expected, further studies should more precisely
288 design the unit of observation intervals in hours to reveal the full process of dynamic loading-induced

289 cellular reactions. Second, in experimental sheep^{43,44} and horse^{45,46} models, lubricin concentration in the
290 synovial fluid was upregulated transiently in the acute phase after injury, and synovial PRG4 (the gene
291 encoding lubricin) expression was positively correlated with TNF α and ADAMTS-5⁴⁶. Future studies
292 should evaluate not only cartilage, but also synovium using quantitative techniques to specify the details
293 of lubricin recovery. Moreover, we did not record the activities of rats after loading that may have
294 influenced the progression of lubricin self-healing, which may have contributed to the large variation in
295 the data (Figure 5D). Third, in the current study, we assessed only the cartilage lesion on the lateral femur
296 condyle, which is not the main part of cartilage loaded during walking⁴⁷. Considering that cartilage
297 heterogeneity could affect the results of injury assessment, cartilage damage on the other contact surface
298 should be examined in the future. Finally, we failed to compare the current model to any surgery-induced
299 model. As described above, the surface lubricin is reportedly diminished in many injury-induced OA
300 animals^{28,34-36}, whereas it is still unknown if joint instability independently affects the progression of post-
301 traumatic OA, especially in the lesion area. Further studies should combine invasive destabilization
302 surgery with preexisting lesions caused by cyclic compression, which could reflect the spatiotemporal
303 changes of cartilage in the non-contact area.

304 In conclusion, we found a specific, localized AC lesion in both the 20 N and 50 N groups that underwent
305 60 cycles of compression in rat knee joints. The local expression of type II collagen was increased after
306 repeated loading, whereas lubricin in the cartilage surface was lost in response to cyclic compression.
307 However, the distribution of superficial lubricin recovered 4 weeks after non-surgical injury (Figure 6).
308 These results indicate that dynamic loading exceeding 20 N damages the lateral femoral condyle AC in
309 rats. Although the damage caused localized chondrocyte death and upregulated expression of degrading
310 enzymes, endogenous repair in well-structured joints rebuilt the layer of protective proteins on the
311 superficial cartilage.

312

313 **Acknowledgments**

314 This study was supported in part by a JSPS KAKENHI Grant, number JP18H03129 and JP18K19739.

315

316 **Author Contributions**317 XJ: conception and design of the study, acquisition, analysis, and interpretation of data, drafting of the
318 article, revision of the article, final approval of the article.319 AI: conception and design of the study, interpretation of data, drafting of the article, revision of the article,
320 final approval of the article.321 AN: conception and design of the study, interpretation of data, revision of the article, and final approval
322 of the article.323 KN: conception and design of the study, interpretation of data, revision of the article, final approval of the
324 article.325 HK: obtaining funding, conception and design of the study, interpretation of data, revision of the article,
326 and final approval of the article.327 TA: conception and design of the study, interpretation of data, revision of the article, and final approval
328 of the article.

329

330 **References**

- 331 1. Kuyinu EL, Narayanan G, Nair LS, et al. Animal models of osteoarthritis: classification, update,
-
- 332 and measurement of outcomes.
- J Orthop Surg Res*
- 2016; 11: 19.
-
- 333 2. De Souza RL, Matsuura M, Eckstein F, et al. Non-invasive axial loading of mouse tibiae increases
-
- 334 cortical bone formation and modifies trabecular organization: a new model to study cortical and
-
- 335 cancellous compartments in a single loaded element.
- Bone*
- 2005; 37: 810-818.
-
- 336 3. Holguin N, Brodt MD, Sanchez ME, et al. Adaptation of tibial structure and strength to axial
-
- 337 compression depends on loading history in both C57BL/6 and BALB/c mice.
- Calcif Tissue Int*
-
- 338 2013; 93: 211-221.
-
- 339 4. Lynch ME, Main RP, Xu Q, et al. Cancellous bone adaptation to tibial compression is not sex
-
- 340 dependent in growing mice.
- J Appl Physiol*
- (1985) 2010; 109: 685-691.
-
- 341 5. Poulet B, Hamilton RW, Shefelbine S, et al. Characterizing a novel and adjustable noninvasive
-
- 342 murine joint loading model.
- Arthritis Rheum*
- 2011; 63: 137-147.
-
- 343 6. Wu P, Holguin N, Silva MJ, et al. Early response of mouse joint tissue to noninvasive knee injury
-
- 344 suggests treatment targets.
- Arthritis Rheumatol*
- 2014; 66: 1256-1265.
-
- 345 7. Lockwood KA, Chu BT, Anderson MJ, et al. Comparison of loading rate-dependent injury modes
-
- 346 in a murine model of post-traumatic osteoarthritis.
- J Orthop Res*
- 2014; 32: 79-88.

- 347 8. Ko FC, Dragomir C, Plumb DA, et al. In vivo cyclic compression causes cartilage degeneration
348 and subchondral bone changes in mouse tibiae. *Arthritis Rheum* 2013; 65: 1569-1578.
- 349 9. Poulet B, de Souza R, Kent AV, et al. Intermittent applied mechanical loading induces subchondral
350 bone thickening that may be intensified locally by contiguous articular cartilage lesions.
351 *Osteoarthritis Cartilage* 2015; 23: 940-948.
- 352 10. Onur TS, Wu R, Chu S, et al. Joint instability and cartilage compression in a mouse model of
353 posttraumatic osteoarthritis. *J Orthop Res* 2014; 32: 318-323.
- 354 11. Ko FC, Dragomir CL, Plumb DA, et al. Progressive cell-mediated changes in articular cartilage
355 and bone in mice are initiated by a single session of controlled cyclic compressive loading. *J*
356 *Orthop Res* 2016; 34: 1941-1949.
- 357 12. Adebayo OO, Ko FC, Wan PT, et al. Role of subchondral bone properties and changes in
358 development of load-induced osteoarthritis in mice. *Osteoarthritis Cartilage* 2017; 25: 2108-2118.
- 359 13. McErlain DD, Appleton CT, Litchfield RB, et al. Study of subchondral bone adaptations in a
360 rodent surgical model of OA using in vivo micro-computed tomography. *Osteoarthritis Cartilage*
361 2008; 16: 458-469.
- 362 14. Iijima H, Aoyama T, Ito A, et al. Destabilization of the medial meniscus leads to subchondral bone
363 defects and site-specific cartilage degeneration in an experimental rat model. *Osteoarthritis*
364 *Cartilage* 2014; 22: 1036-1043.
- 365 15. Bomsta BD, Bridgewater LC, Seegmiller RE. Premature osteoarthritis in the Disproportionate
366 micromelia (Dmm) mouse. *Osteoarthritis Cartilage* 2006; 14: 477-485.
- 367 16. Iijima H, Aoyama T, Ito A, et al. Effects of short-term gentle treadmill walking on subchondral
368 bone in a rat model of instability-induced osteoarthritis. *Osteoarthritis Cartilage* 2015; 23: 1563-
369 1574.
- 370 17. Hayami T, Pickarski M, Wesolowski GA, et al. The role of subchondral bone remodeling in
371 osteoarthritis: reduction of cartilage degeneration and prevention of osteophyte formation by
372 alendronate in the rat anterior cruciate ligament transection model. *Arthritis Rheum* 2004; 50:
373 1193-1206.
- 374 18. Iijima H, Aoyama T, Tajino J, et al. Subchondral plate porosity colocalizes with the point of
375 mechanical load during ambulation in a rat knee model of post-traumatic osteoarthritis.
376 *Osteoarthritis Cartilage* 2016; 24: 354-363.
- 377 19. Wong M, Carter DR. Articular cartilage functional histomorphology and mechanobiology: a
378 research perspective. *Bone* 2003; 33: 1-13.
- 379 20. Jeon JE, Schrobback K, Hutmacher DW, et al. Dynamic compression improves biosynthesis of
380 human zonal chondrocytes from osteoarthritis patients. *Osteoarthritis Cartilage* 2012; 20: 906-915.
- 381 21. Jorgensen AEM, Kjaer M, Heinemeier KM. The Effect of Aging and Mechanical Loading on the
382 Metabolism of Articular Cartilage. *J Rheumatol* 2017; 44: 410-417.
- 383 22. Glasson SS, Askew R, Sheppard B, et al. Deletion of active ADAMTS5 prevents cartilage
384 degradation in a murine model of osteoarthritis. *Nature* 2005; 434: 644-648.
- 385 23. Ragan PM, Badger AM, Cook M, et al. Down-regulation of chondrocyte aggrecan and type-II
386 collagen gene expression correlates with increases in static compression magnitude and duration.
387 *J Orthop Res* 1999; 17: 836-842.
- 388 24. Fitzgerald JB, Jin M, Dean D, et al. Mechanical compression of cartilage explants induces multiple
389 time-dependent gene expression patterns and involves intracellular calcium and cyclic AMP. *J*
390 *Biol Chem* 2004; 279: 19502-19511.
- 391 25. Anderson DE, Johnstone B. Dynamic Mechanical Compression of Chondrocytes for Tissue
392 Engineering: A Critical Review. *Front Bioeng Biotechnol* 2017; 5: 76.

- 393 26. Yamaguchi S, Aoyama T, Ito A, et al. The Effect of Exercise on the Early Stages of Mesenchymal
394 Stromal Cell-Induced Cartilage Repair in a Rat Osteochondral Defect Model. *PLoS One* 2016; 11:
395 e0151580.
- 396 27. Coles JM, Zhang L, Blum JJ, et al. Loss of cartilage structure, stiffness, and frictional properties
397 in mice lacking PRG4. *Arthritis Rheum* 2010; 62: 1666-1674.
- 398 28. Elsaid KA, Machan JT, Waller K, et al. The impact of anterior cruciate ligament injury on lubricin
399 metabolism and the effect of inhibiting tumor necrosis factor alpha on chondroprotection in an
400 animal model. *Arthritis Rheum* 2009; 60: 2997-3006.
- 401 29. Jones AR, Chen S, Chai DH, et al. Modulation of lubricin biosynthesis and tissue surface
402 properties following cartilage mechanical injury. *Arthritis Rheum* 2009; 60: 133-142.
- 403 30. McCann L, Ingham E, Jin Z, et al. Influence of the meniscus on friction and degradation of
404 cartilage in the natural knee joint. *Osteoarthritis Cartilage* 2009; 17: 995-1000.
- 405 31. Drewniak EI, Jay GD, Fleming BC, et al. Cyclic loading increases friction and changes cartilage
406 surface integrity in lubricin-mutant mouse knees. *Arthritis Rheum* 2012; 64: 465-473.
- 407 32. Neu CP, Reddi AH, Komvopoulos K, et al. Increased friction coefficient and superficial zone
408 protein expression in patients with advanced osteoarthritis. *Arthritis Rheum* 2010; 62: 2680-2687.
- 409 33. Elsaid KA, Fleming BC, Oksendahl HL, et al. Decreased lubricin concentrations and markers of
410 joint inflammation in the synovial fluid of patients with anterior cruciate ligament injury. *Arthritis*
411 *Rheum* 2008; 58: 1707-1715.
- 412 34. Wei L, Fleming BC, Sun X, et al. Comparison of differential biomarkers of osteoarthritis with and
413 without posttraumatic injury in the Hartley guinea pig model. *J Orthop Res* 2010; 28: 900-906.
- 414 35. Flannery CR, Zollner R, Corcoran C, et al. Prevention of cartilage degeneration in a rat model of
415 osteoarthritis by intraarticular treatment with recombinant lubricin. *Arthritis Rheum* 2009; 60:
416 840-847.
- 417 36. Young AA, McLennan S, Smith MM, et al. Proteoglycan 4 downregulation in a sheep
418 meniscectomy model of early osteoarthritis. *Arthritis Res Ther* 2006; 8: R41.
- 419 37. Elsaid KA, Zhang L, Waller K, et al. The impact of forced joint exercise on lubricin biosynthesis
420 from articular cartilage following ACL transection and intra-articular lubricin's effect in exercised
421 joints following ACL transection. *Osteoarthritis Cartilage* 2012; 20: 940-948.
- 422 38. Teeple E, Jay GD, Elsaid KA, et al. Animal models of osteoarthritis: challenges of model selection
423 and analysis. *Aaps j* 2013; 15: 438-446.
- 424 39. Vugmeyster Y, Wang Q, Xu X, et al. Disposition of human recombinant lubricin in naive rats and
425 in a rat model of post-traumatic arthritis after intra-articular or intravenous administration. *Aaps j*
426 2012; 14: 97-104.
- 427 40. Jay GD, Fleming BC, Watkins BA, et al. Prevention of cartilage degeneration and restoration of
428 chondroprotection by lubricin tribosupplementation in the rat following anterior cruciate ligament
429 transection. *Arthritis Rheum* 2010; 62: 2382-2391.
- 430 41. Nugent GE, Aneloski NM, Schmidt TA, et al. Dynamic shear stimulation of bovine cartilage
431 biosynthesis of proteoglycan 4. *Arthritis Rheum* 2006; 54: 1888-1896.
- 432 42. Schatti OR, Markova M, Torzilli PA, et al. Mechanical Loading of Cartilage Explants with
433 Compression and Sliding Motion Modulates Gene Expression of Lubricin and Catabolic Enzymes.
434 *Cartilage* 2015; 6: 185-193.
- 435 43. Barton KI, Ludwig TE, Achari Y, et al. Characterization of proteoglycan 4 and hyaluronan
436 composition and lubrication function of ovine synovial fluid following knee surgery. *J Orthop Res*
437 2013; 31: 1549-1554.

- 438 44. Atarod M, Ludwig TE, Frank CB, et al. Cartilage boundary lubrication of ovine synovial fluid
439 following anterior cruciate ligament transection: a longitudinal study. *Osteoarthritis Cartilage*
440 2015; 23: 640-647.
- 441 45. Antonacci JM, Schmidt TA, Serventi LA, et al. Effects of equine joint injury on boundary
442 lubrication of articular cartilage by synovial fluid: role of hyaluronan. *Arthritis Rheum* 2012; 64:
443 2917-2926.
- 444 46. Reesink HL, Watts AE, Mohammed HO, et al. Lubricin/proteoglycan 4 increases in both
445 experimental and naturally occurring equine osteoarthritis. *Osteoarthritis Cartilage* 2017; 25: 128-
446 137.
- 447 47. Zevenbergen L, Smith CR, Van Rossom S, et al. 2018. Cartilage defect location and stiffness
448 predispose the tibiofemoral joint to aberrant loading conditions during stance phase of gait. *PloS*
449 *one* 13:e0205842.
- 450
- 451
- 452
- 453
- 454
- 455
- 456
- 457
- 458
- 459
- 460
- 461
- 462
- 463
- 464
- 465
- 466
- 467
- 468
- 469
- 470
- 471

472 **Figure legends**

473

474 **Figure 1.** Schematic diagram of the non-surgical cyclic compression model. **A.** Right knee of anesthetized
475 rat fixed on a customized apparatus with the patella embedded in a loading dent. The indexed knee angle
476 was set at a deep flexion of 140°. **B.** A full cycle of the loading regimen contained a 0.5 s peak load and a
477 10 s rest interval with the loading cup approaching at a speed of 1 mm/s. The preload of 5 N and peak load
478 of 20 N or 50 N were set for samples in corresponding groups. **C.** Flow chart of sample allocation.

479

480 **Figure 2.** Chondrocyte vitality in superficial cartilage after 20 N compressive loading detection by calcein
481 AM/ethd-1 staining. Representative fluorescent images demonstrate spatiotemporal cell death from 1 to
482 12 h after loading. Green and red channels illustrate the distribution of live and dead chondrocytes,
483 respectively. A well-defined focal region without green-stained cells was observed at 6 and 12 h. Pre-
484 loaded normal rat limbs were used as controls. Scale bar: 100 µm.

485

486 **Figure 3.** Changes in type II collagen expression in articular cartilage substrates after cyclic loading. **A.**
487 Representative immunostained sections for type II collagen in the lesion areas of lateral condyle cartilage.
488 The border of normal and degenerative cartilage is represented by a dashed, light-gray line. **B.** Differences
489 in type II collagen expression in control and loaded samples. **C.** Average intensity of staining on the
490 degenerative cartilage matrix was calculated on 8-bit grayscale images using ImageJ software. **D.**
491 Percentage variation of intensity in the lesion area relative to the intact area on the same section. Relative
492 intensity was calculated in an inverted 8-bit grayscale image by dividing the intensity in the intact area.
493 Significant effect or interaction between time points or load levels; ** $p < 0.01$. No symbol: not significant.
494 Scale bar: 100 µm.

495

496 **Figure 4.** The distribution of MMP-13⁺ chondrocytes in articular cartilage. **A.** Representative histological
497 sections immunostained for MMP-13⁺ in the lesion area and the adjoining zone. Black arrow heads
498 indicate positive cells in the superficial and intermediate zone of cartilage, red arrow heads indicate
499 positive cells under the tidemark. **B.** Comparison of positive cell number in intact cartilage with all loaded
500 samples' adjoining area. **C, D.** Results of semi-quantitative analyses of positive cells within the adjoining
501 (C) and under the lesion area (D). Results were normalized by dividing by the cartilage surface length
502 (mm). Significant results ($p < 0.05$) of ANOVA analysis ‡: main effect of duration was presented on the
503 top of each chart. Marginal means of each observational point were compared when ‡ was found. * $p < 0.05$,
504 ** $p < 0.01$. Scale bar: 100 µm.

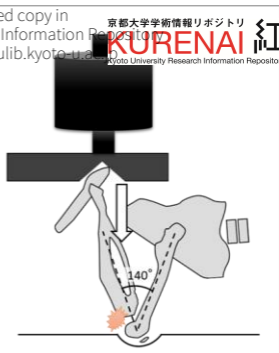
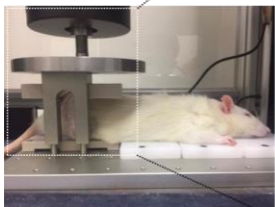
505

506 **Figure 5.** Localization of lubricin in articular cartilage subjected to dynamic loading. **A.** Representative
507 Lubricin/Proteoglycan4 immunostained image in the lesion area of lateral condyle and intact area under
508 the lateral meniscus. Staining was weakened in the superficial substrates, whereas it was enhanced in the
509 cartilage lacunae. **B.** Differences between control (n=6), early observation (3 days and 1 week; n=24), and

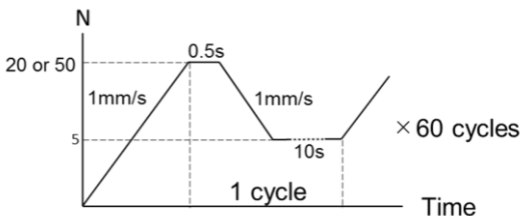
510 later observation (2, 4, and 8 weeks; n=36) of loaded samples were compared using Kruskal-Wallis H
 511 tests. **C.** Staining intensity in the superficial layer of cartilage substrates. The ROI of superficial cartilage
 512 were depicted with ImageJ software using the brush selection tool with 50 μm width (Supplementary
 513 figure 3). **D.** Relative intensity normalized with intact region staining in percentage. Significant results
 514 ($p<0.05$) of a two-way ANOVA are presented on the top of each chart; ‡: main effect of duration, Ψ :
 515 interaction effects. Stratified one-way ANOVA on each load level with multiple comparison were applied
 516 whenever Ψ was found. * $p<0.05$, ** $p<0.01$. No symbol: not significant. Scale bar: 100 μm .

517

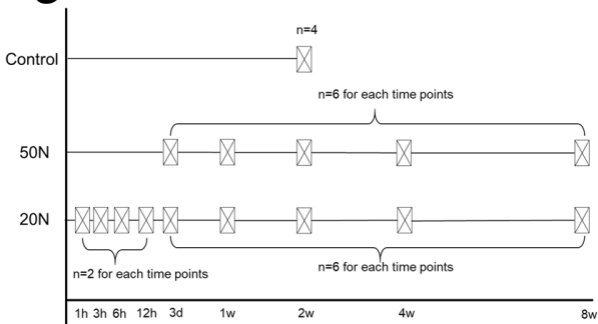
518 **Figure 6.** The illustration summarizes the findings of the current study. Localized Col2 was upregulated
 519 within 3 days after loading and stable during observation. Superficial lubricin decreased immediately after
 520 damage yet recovered gradually to the normal level. Safranin O staining in lesion cartilage weakened
 521 continuously after injury until week 4. Hematoxylin-stained nuclei in the damaged area dissolved
 522 completely 2 weeks after cyclic compression.



B



C



: Animal sacrifice

Figure 1



Control

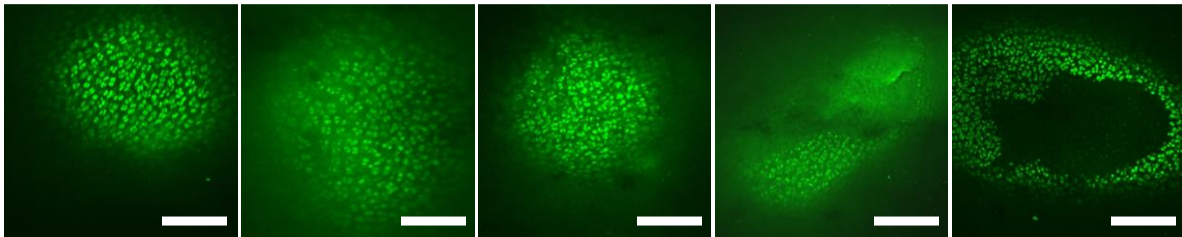
1 hour

3 hours

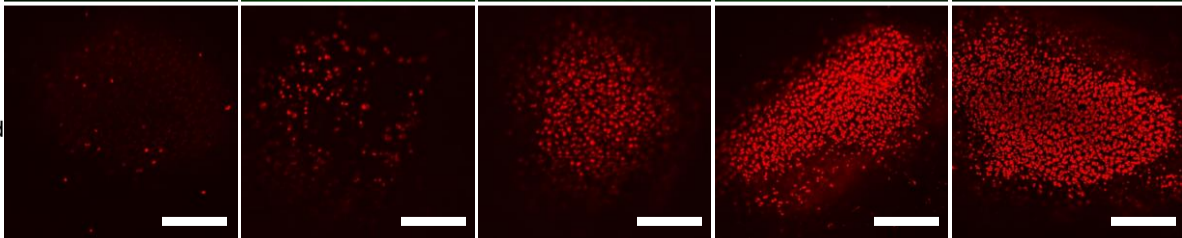
6 hours

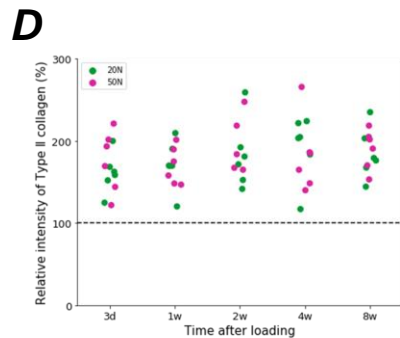
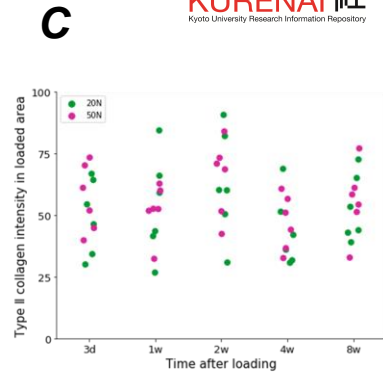
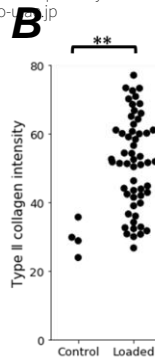
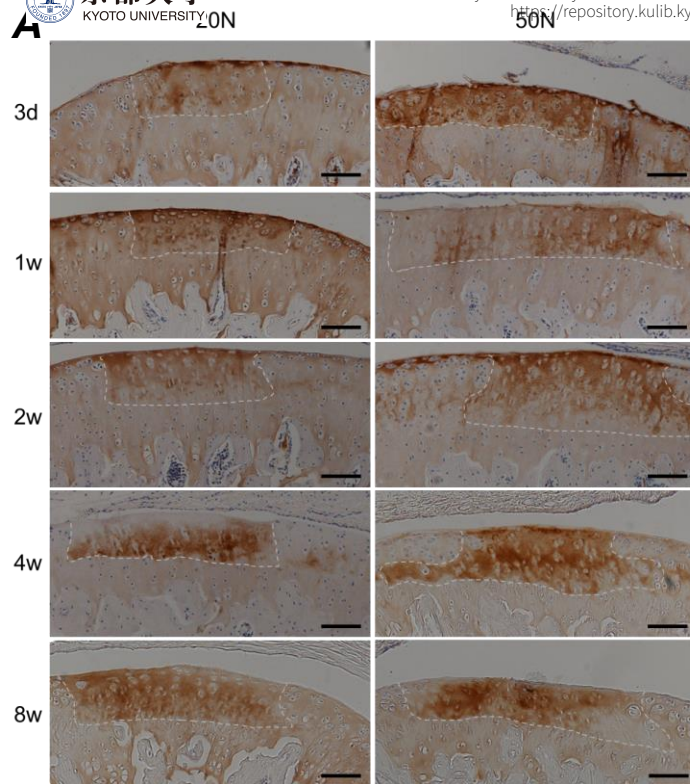
12 hours

Live



Dead





Adjoining area

Lesion area

Adjoining area

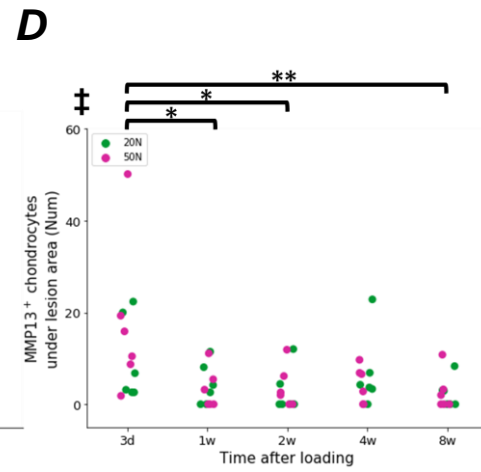
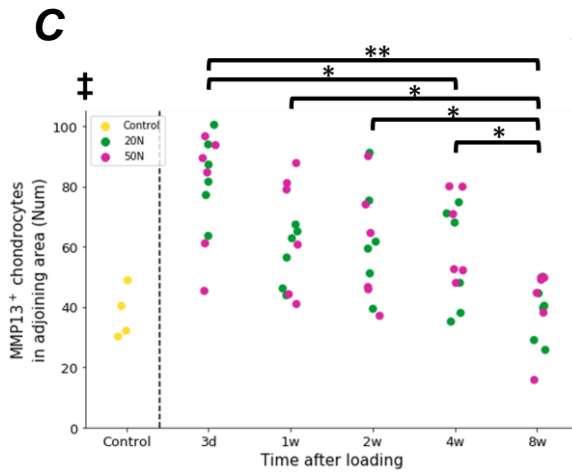
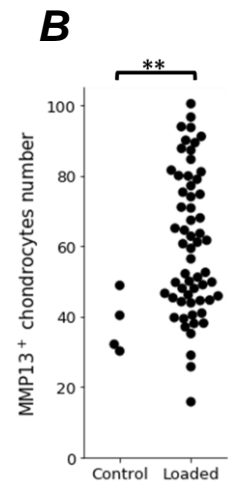
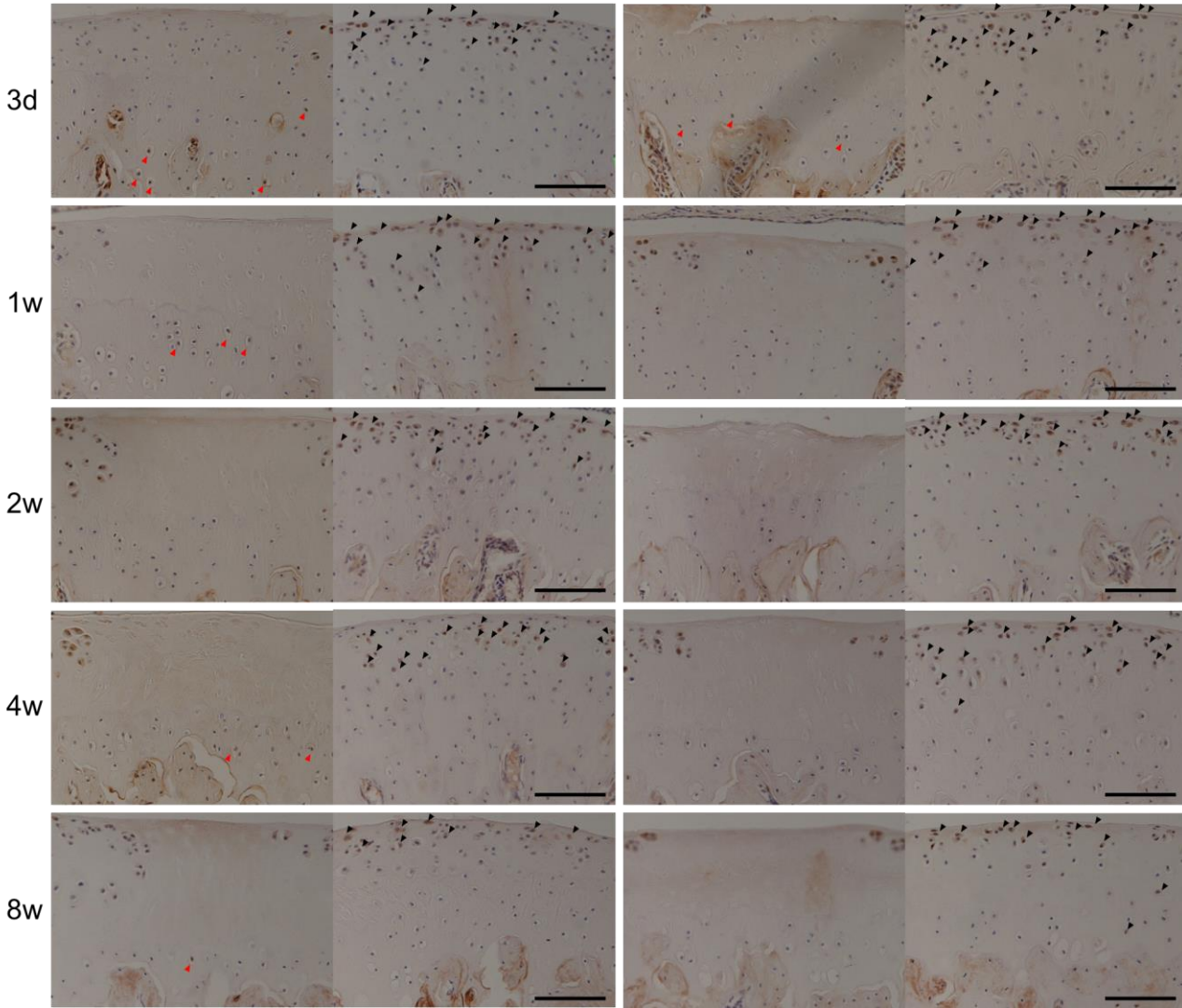


Figure 4

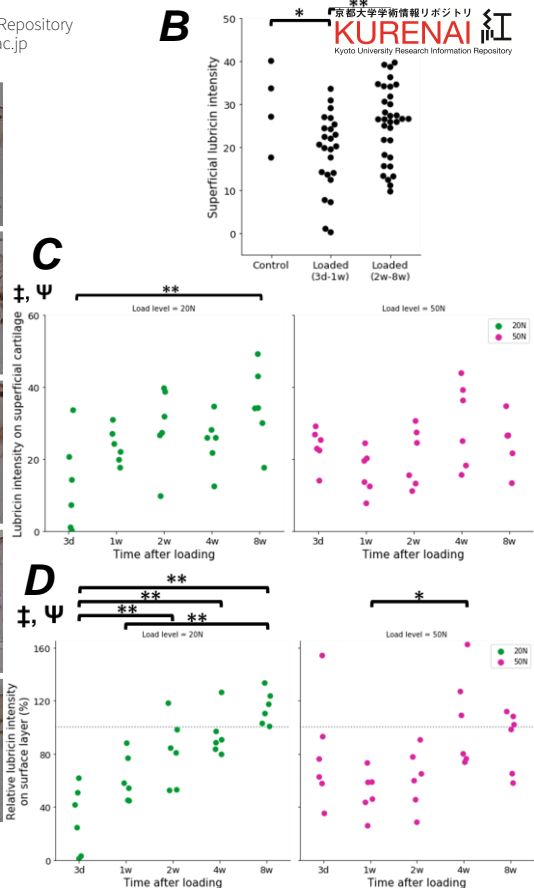
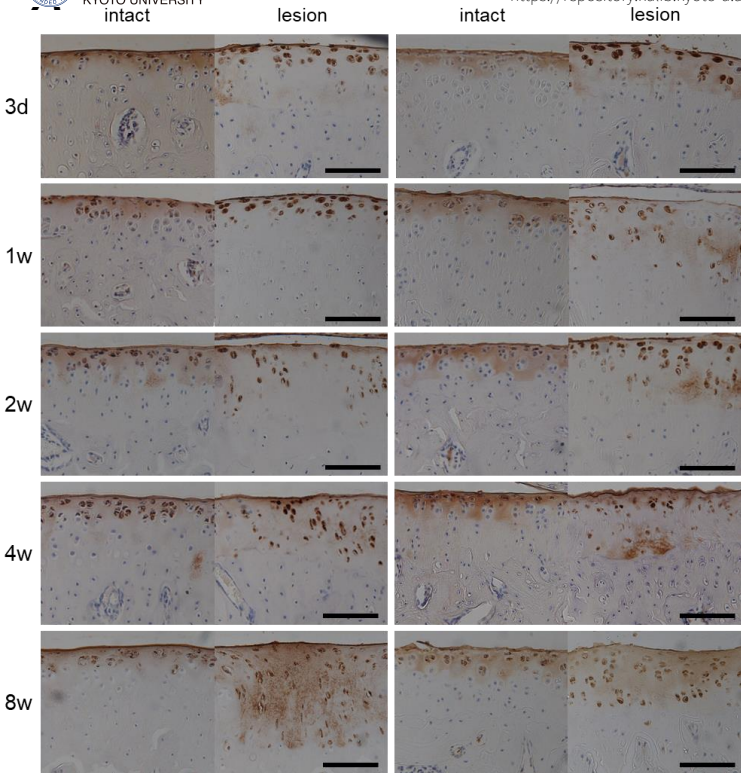


Figure 5

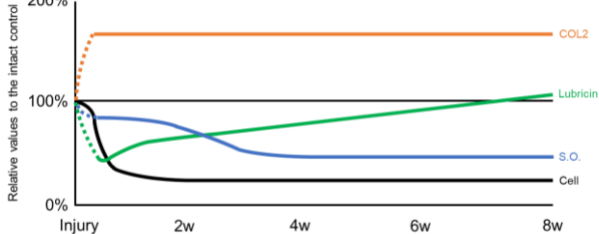


Figure 6